Telescope Mirror Contamination and Airborne Dust

J. R. Varsik, W. A. Siegmund, and D. H. Berger

August 20, 1997

Abstract

Airborne particulate matter (dust) is a major contaminant of telescope optics. In support of an initiative to study a large reflecting coronagraph, a project to monitor airborne dust and its deposition on mirror surfaces has begun. High airborne dust concentrations at Sacramento Peak are episodic in nature; each episode lasting several hours. Occurrence of dust episodes is determined by local climatic conditions. During these episodes, the concentration of larger particles increases disproportionately. Surface dust measurements indicate that the particles that contribute most to the scattering of light from optical surfaces are larger than those that dominate scattering in the air. Comparisons of surface particle densities measured from sample slides and the airborne dust counts suggest criteria for operation of telescopes in the Sacramento Peak area.

1 Introduction

Airborne particulate matter is a major contaminant of telescope optical surfaces. This is particularly a problem for coronagraphic telescopes, which require scattered light on the order of a few millionths of the brightness of the solar disk only a few arcseconds above the limb of the Sun. In addition, future solar work will emphasize the near infrared, where the emissivity of these particles will also act as a limit to the sensitivity of the telescope. Therefore, such an instrument must be placed in a clean site and must be kept very clean.

For nighttime telescopes, the effect of dust on mirror surfaces on the PSF is more subtle. The contribution of dust to the PSF of a stellar source occurs mainly at large angles ($\sim 10^3$ arcseconds) so is not of immediate concern to stellar astronomers. However, the sky background level is increased significantly even several degrees from a bright star. In addition, the light scattered by dust on the primary mirror becomes the major component of the total light scatted by the telescope. This makes the baffling requirements for a nighttime telescope much more stringent than they would otherwise be (Kuhn, 1997).

For all telescopes, contamination of optical surfaces reduces throughput, sometimes by rather large amounts (see section 4.3 below), and emissivity in the infrared is also a problem. For non-solar coronagraphic work (e.g. close binary stars, extrasolar planets) scattered light imposes significant limits on observations because of its contribution to the point-spread function (PSF). Therefore, scattered light reduction should be an important consideration in the design and operation of telescopes in general.

In this paper we will refer to all forms of airborne particulate matter (organic and inorganic), as well as particulate matter on mirror surfaces, as "dust". There are two aspects to the experiment: monitoring airborne dust and monitoring surface dust. Airborne dust degrades solar observations in two ways: first by scattering of sunlight in the atmosphere before light enters the telescope and second by depositing particles on optical surfaces in the telescope. The second effect is much greater than the first, but both are significant.

An earlier experiment in airborne dust monitoring by Giordano and Sarazin (1994) at Cerro Paranal showed that at that site although dust levels are generally low pulses of high dust concentration occur that last from hours to days. Anecdotal evidence from Sacramento Peak suggested similar conditions occur there. One purpose of our experiment was to collect objective data on these dust events.

2 Data and Experiment Design

2.1 The Airborne Dust Counter

This experiment is intended to monitor airborne dust levels for a period of at least several months for comparison with other weather data and coronal sky brightness measurements. The information will ultimately be used for determining the degree of dust control necessary for the CLEAR telescope (Beckers 1996) and the suitability of possible telescope sites. The initial objectives of this experiment include:

- A search for seasonal variations in airborne dust.
- Measurement of the properties of dust episodes. These are events reported by the observing staff at Sacramento Peak and Apache Point in which visibility is reduced. We are interested in how objective dust measurements correlate with these observer reports.

The dust counter used for this experiment was purchased for the Sloan Digital Sky Survey scattered light and mirror contamination study. Apache Point Observatory was also interested in setting up a dust monitor for the purpose of providing more environmental information to their remote observers, so that the astronomers observing remotely would have some objective information about dust levels instead of relying on the staff observer's subjective measurements. APO also had a weather mast with power and data connections available. Therefore we decided initially to mount the dust monitor provided by APO on the APO weather mast. Measurements are made at 15-minute intervals, and are accessible on the APO WWW site. The data are also recorded in a log file for each day.

The initial data acquisition system, based on a 80386 PC, was built at NSO/SP. Initial tests of remote control of the dust counter were made at NSO/SP, additionally the weather-tight enclosure was assembled there. Once the dust counter was mounted on the APO weather mast, J. R. Fowler of APO modified the existing APO weather-logging software to control the dust counter and record the dust count data.

The dust counter is a small portable unit, the Met One (Grants Pass, OR) Model 227B. It works by drawing air through a tube into the counter, where photodiodes measure the light produced by a diode laser and scattered by the dust particles. The air pump draws 0.0028m^3 (0.1 cubic foot) of air per minute through the counter. The counter is automatically run for one minute every 15 minutes. Therefore to obtain the number of particles per cubic meter one multiplies the raw counts by 353.147. The counter has two channels; the lower channel counts particles greater than or equal to 0.3μm in size. The threshold of the upper channel of the airborne dust monitor is adjustable and can be set to 0.5, 1.0, 3.0, or 5.0μm.

The counter is mounted in a weather-tight enclosure (Figure 1) at a height of 15 m on the APO weather mast. This places the instrument in the free air flow, away from the effects of most human activities. It also places the counter at roughly the height above ground for the proposed CLEAR telescope.

The counter has an RS-232 interface and can be controlled by an external computer. For protection from surges caused by storms a fiber optic cable is used, with an appropriate converter mounted in the enclosure with the counter. The fiber optic cable is connected to a terminal server in the APO computer room.

2.2 The Surface Dust Measurement Apparatus

This experiment is intended to examine the number and size distribution of dust particles on glass surfaces. We hope to compare these data with scattering data and data on airborne dust in a search for answers to some of the following questions:

- What size of dust particles contribute to optical scattering?
- What is the size distribution of particles on a surface, and how does it relate to the size distribution of airborne particles?
- Does cleaning the surface preferentially remove certain sized particles?

Figure 1: The Met One dust counter mounted in its weather-tight enclosure. The ports on the bottom of the enclosure for the armored power cable, the fiber optic cables, and the isokinetic dust probe can be seen.

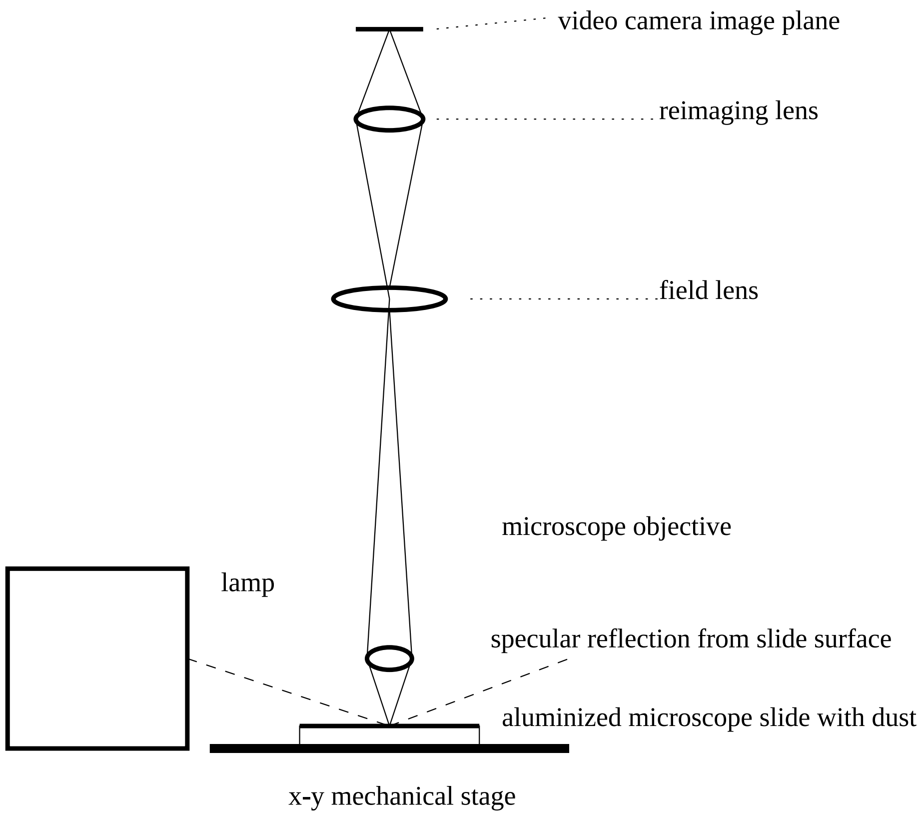

Figure 2: The optical arrangement of the apparatus for the surface dust experiment.

The test surfaces used for this experiment are aluminized microscope slides. Each slide is exposed for one week, after CO_2 cleaning on the mirror cell. Occasionally each slide will be cleaned with alcohol to obtain a reference reading.

Figure 2 shows the optical arrangement of the surface dust experiment. The apparatus consists of a Bushnell microscope with a 10x objective lens and mechanical stage, an Edmund Scientific video adapter (containing the field and reimaging lenses) and a video CCD camera. A simple light bulb is used for illumination. For nearly the entire period discussed here an RCA CCD video camera was used; for a short time (10/3 to 10/15) an NEC model TI-50ES camera was used.

The system works by digitizing video images. The output from the video camera is routed to an 8-bit Imaging Technology frame grabber board in a standard 80386 PC. The system saves digitized images to floppy disk. The images are then processed on the Sacramento Peak Sun network by a computer

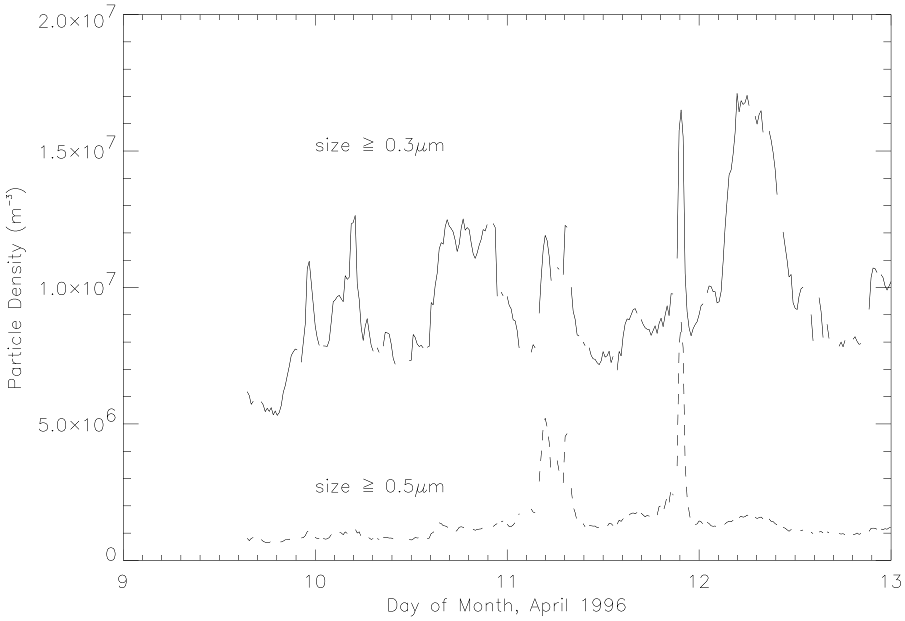

Figure 3: The initial data from the APO weather mast.

program written in the IDL language which determines the number and size distribution of the particles. Eight images at different locations are obtained at each time a slide is measured; the results for the number and size distribution of particles on each slide are averaged.

3 Results

3.1 The Airborne Dust Counter

The dust counter was mounted on the APO weather mast April 9. Initially we set the upper channel to count 0.5μm and larger particles. This setting was used between April 9 to May 6, 1996. The first data from the APO weather mast (Figure 3) showed immediately that the two dust channels were not moving in parallel with each other.

In order to obtain a better estimate of the particle size distribution, we decided that it would be better to have as large a difference between the two particle size channels as possible consistent with reasonable counting statistics and time resolution. Therefore on May 7 we set the upper channel on the counter to 1.0μm and above.

3.2 High Dust Count Events and Visual Observations

High dust levels can affect the amount of observing time available for a telescope. At present in order to prevent excessive mirror contamination, APO closes their 3.5 m telescope when the night assistants see dust particles in a flashlight beam. An analysis was performed on the relationship between high dust counts observed in the MetOne dust counter on the weather tower at APO and dust events reported in the APO night logs by the observers in the spring and early summer of 1996. The period covered is between May 7 and December 31. The upper channel on the dust counter was set to count particles with diameter greater than or equal to 1.0μm on May 7. During the period there were 12 reports of dust events in the APO night logs. Of these, 9 corresponded to particle densities in the $\geq 1.0\mu$m channel of above 1.24×10^6m^{-3} (35000 particles per cubic foot). One event did not correspond to a peak in the $\geq 1.0\mu$m channel, but did correspond to a peak ($\sim 1 \times 10^8$m^{-3} [$\sim 3 \times 10^6$ particles/cubic foot]) in the $\geq 0.3\mu$m channel. Two events, reported on 6/22 at 0100 to 0200 annd on 6/23 at 0200 to 0300, do not correspond to high counts in either dust channel.

Of the three dust events noted in the APO night logs that did not correspond to high particle density in the $\geq 1.0\mu$m channel two also had the notation "smoke" or "smoke/ash". Smoke particles tend to be smaller than 1 micron, so it is reasonable that the $\geq 1.0\mu$m channel on the counter did not detect them. One of these events (on 6/20) corresponds to the 1×10^8m^{-3} peak noted above.

There are problems correlating the exact times from the counter dataset with the observing logs due to a data dropout problem which existed during the early part (May to August 15) of this period. We believe, however, that the correlations we have made between the counter peaks and dust events are reasonable.

It is reasonable to conclude that particle density greater than 1.24×10^6m^{-3} (35000 particles/cubic foot) in the $\geq 1.0\mu$m channel always corresponds to a reportable dust event. Therefore, one might use such a value as a limit for observing. However, not all dust events correspond to such a value. Some dust events appear to be primarily small particles which the $\geq 1.0\mu$m channel on the dust counter does not detect.

Three other events with particle density greater than 1.24×10^6m^{-3} were also recorded by the counter; these periods appear to have been during the day, and so were not noted in the APO night logs.

Ninteen large peaks, greater than 7.1×10^7m^{-3} (2×10^6 particles/cubic foot), were observed in the $\geq 0.3\mu$m channel. Of these, three were associated with dust events noted by the APO observers. Seven events occurred during clouds or high humidity when the telescope was closed. Six events occurred during the day. During two events there were clouds for part of the duration of the event, but the telescope was open during part of the event. One event is not accounted for in the observing logs. Visible dust events did not occur between the nights

Date	Time Range	0.3μm (m^{-3})	1.0μm (m^{-3})	Duration (hr)	n
14 May	02:00 - 10:00	6.18×10^7	8.95×10^5	8.0	-3.52
24 May	23:00 - 00:00	2.55×10^7	9.55×10^5	1.0	-2.73
25 May	20:00 - 00:00	5.09×10^7	1.38×10^6	4.0	-3.00
08 Jun.	00:45 - 02:00	3.59×10^7	1.26×10^6	1.25	-2.78
09 Jun.	07:00 - 11:00*	2.10×10^7	3.68×10^6	4.0	-1.44
10 Jun.	08:30 - 11:00*	3.27×10^7	3.05×10^6	2.5	-1.97
21 Jun.	00:00 - 05:00	7.89×10^7	1.36×10^5	5.0	-5.28
22 Jun.	01:30 - 03:00	2.24×10^7	6.70×10^4	1.5	-4.83
23 Jun.	01:00 - 03:00*	1.47×10^7	9.50×10^4	2.0	-4.19
24 Jun.	19:00 - 01:00	3.02×10^7	7.90×10^6	6.0	-1.11
25 Oct.	17:00 - 05:00	1.47×10^7	2.77×10^6	12.0	-1.38
16 Nov.	03:30 - 05:00	1.14×10^7	1.09×10^6	1.5	-1.06

Table 1: Characteristics of logged dust events, May 7 to Dec. 31 1996. The * indicates problems with data dropouts in determining the exact time of events from the dust counter data, or times determined from the observing logs.

Average n for all events seen in 1.0μm channel	-2.21
Average n for all events	-2.85
Average duration of events seen in 1.0μm channel	4.5 hr
Average duration of all events	4.1 hr
Overall average count, 0.3 μm channel, 1.0μm events	$3.16 \times 10^7 m^{-3}$
Ovarall average count, 1.0 μm channel, 1.0μm events	$2.55 \times 10^6 m^{-3}$
Overall average count, 0.3 μm channel, all events	$3.33 \times 10^7 m^{-3}$
Overall average count, 1.0 μm channel, all events	$1.94 \times 10^6 m^{-3}$

Table 2: Statistics on dust events logged by APO observers. Events with density $\geq 1.24 \times 10^6 m^{-3}$ in the 1.0μm channel are noted as "seen in 1.0μm channel".

of June 24/25 and October 25/26, 1996. A software problem caused data to be lost the weekend of August 10, otherwise the system has been able to operate continuously.

Just as the 0.3 micron channel turned out to not necessarily represent well the results at 1 micron, we can expect that dust density measurements in the 3 to 10 micron region will be different from what we might expect based on the 1 micron measurements. It would be useful to obtain such measurements, but this will require a different instrument from the existing one because the low abundance of such particles requires sampling much more air than the current counter can process.

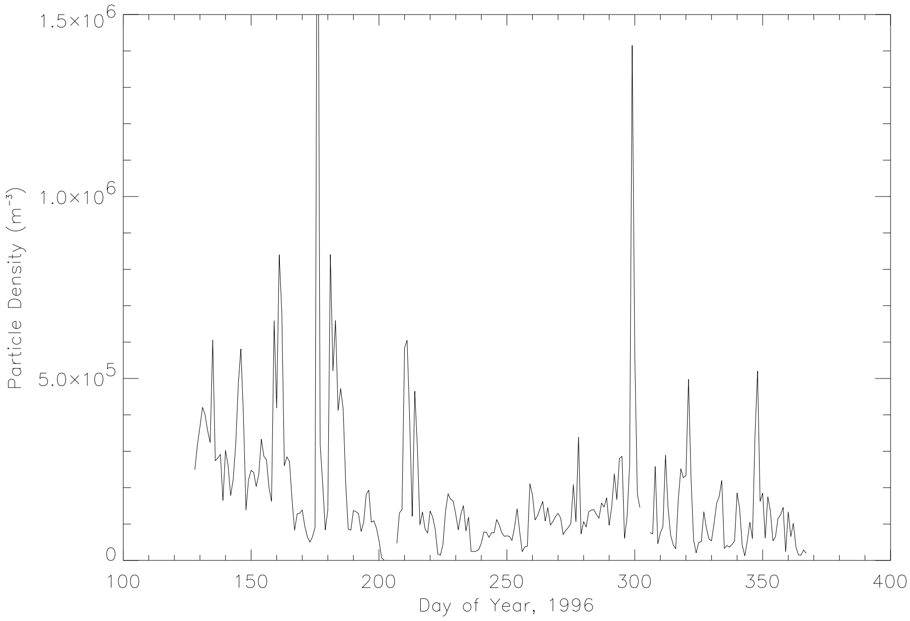

Figure 4: Daily average dust levels in the $\geq 1.0\mu$m channel for the May 7 to December 31, 1996 period.

3.3 Seasonal Variations in Airborne Dust Counts

The daily average dust levels for the two channels are shown in Figures 4 and 5. There appear to be three different "seasons" for dust levels at Sacramento Peak. The first has begun by the beginning of May and lasts until the end of June (day-of-year 181). In this period the average dust level is high and there are a large number of dust events. The second period more-or-less corresponds to the "monsoon season" in the southwest U.S., when the weather is influenced by upper-level low pressure systems coming from the south. This period runs from the beginning of July to the end of September (day-of-year 273). Dust levels are low for this period, and there are few visible dust events. Thunderstorms are frequent in mountainous areas during this time. The third "season" runs from the beginning of October to at least the end of the year. Average dust levels during this period are low, but there is greater variability than during the "monsoon" period.

This suggests that the size distribution of particles is varying, and does not correspond to the standard value given by the formula of McClatchey et al. (1978) of y^{-4}, where y is the particle diameter. Since we have two size channels with our dust counter, we can estimate the particle size distribution.

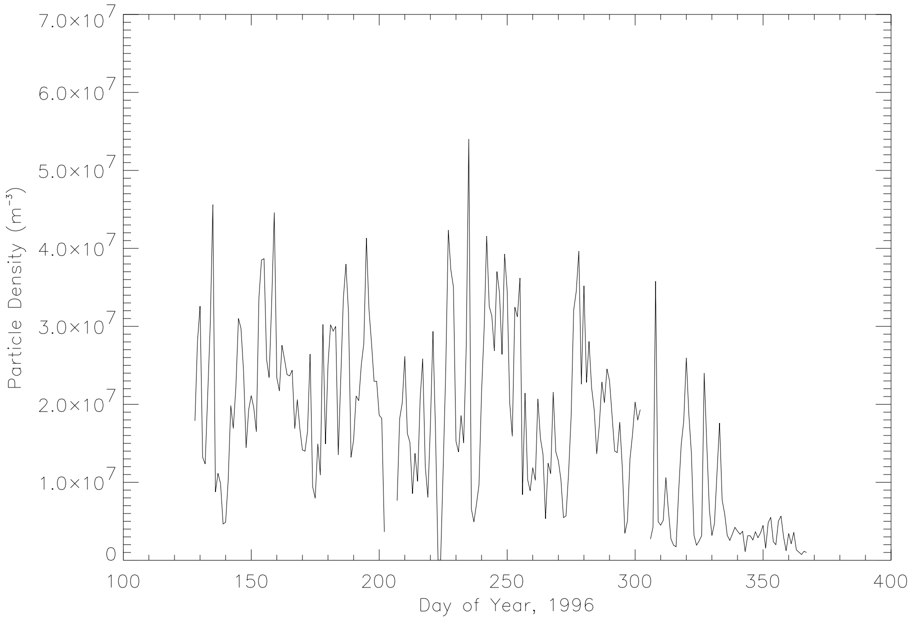

Figure 5: Daily average dust levels in the $\geq 0.3\mu$m channel for the May 7 to December 31, 1996 period.

Let $N(y)$ be the particle number density (number of particles of diameter y per cubic meter) and let $M(y)$ be the cumulative density (number of particles with diameter $\geq y$, the quantity the counter measures). Then, assuming a relation of the form

$$N(y) = Ky^m$$

we can find for $m < -1$

$$M(y) = \frac{K}{-1(m+1)} y^{m+1}$$

or, if we let $n = m + 1$,

$$M(y) = K' y^n.$$

n can be estimated given the cumulative density at two diameters.

Figure 6 shows the exponent n for the period from May 7 to December 31, using the $\geq 0.3\mu$m and $\geq 1.0\mu$m channels. While the exponent n is close to -4 much of the time, there are times when we have a much larger number of large particles relative to the small ones. The density at times is proportional to y^{-2} and and at one time appeared even flatter. These flatter distributions correspond much of the time to high counts in the larger than 1.0μm channel, but not always.

This result may help us get a better correlation between the dust counts and the reports of dust in the flashlight beams at night. The observers are probably seeing fairly large particles ($\sim 10\mu$m). The number of such particles will be strongly affected by the value of n.

Average particle counts were determined for the three "seasons" described above as well as for three periods at Cerro Paranal, using data provided by Sarazin and Giordano (1997). The average value of n was determined for both sites and is also given in Table 3.

We then find that at Sacramento Peak $|n|$ is higher in monsoon season (7/1 to 9/30), lower outside of monsoon season. The average particle counts indicate that even though the number of large particles dropped during monsoon season, the number of small particles remained high.

At Cerro Paranal, the number of small particles is similar to that at Sacramento Peak, but the number of large particles during the February to July (Chilean fall and winter) period is much lower than at Sacramento Peak, even during the Sacramento Peak monsoon period.

We find that n also varies on short timescales. During dust events, n increases, indicating that the increase in the number of $\geq 1.0\mu$m particles is much greater than that for the $\geq 0.3\mu$m particles. These short term variations in n (and the visible dust events) were not associated with obvious variations in local weather conditions. However, on a longer-term basis, a correlation exists between average dust levels in the $\geq 1.0\mu$m channel and relative humidity, both

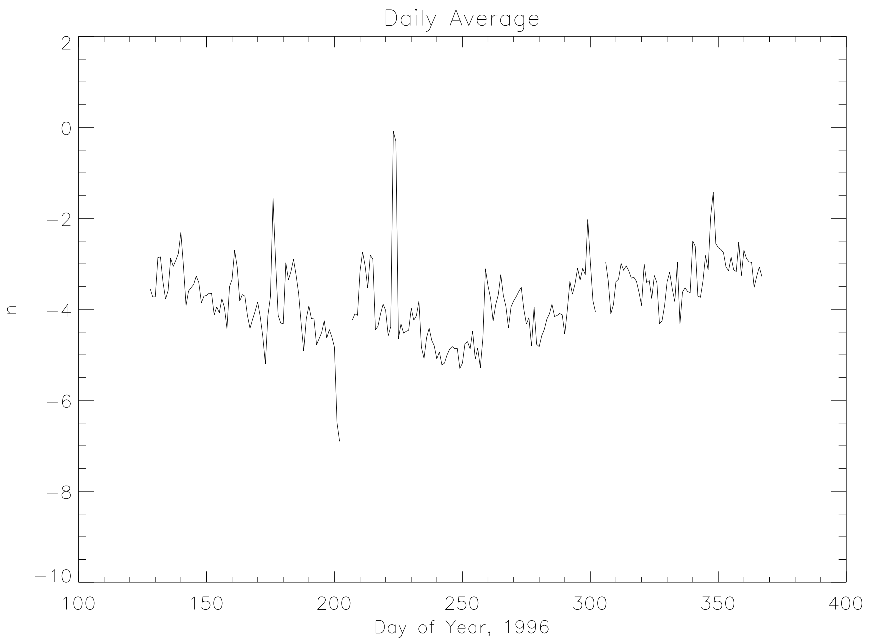

Figure 6: The value of the daily average of n, the power law exponent of the particle size distribution, for dust counts from the APO weather mast, versus the day of the year for 1996. The data cover the period from May 7 to December 31.

Season	$\geq 0.3\mu$m channel (m^{-3})	$\geq 1.0\mu$m channel (m^{-3})	n
Sac Peak Averages for 1996			
Spring (5/7 to 6/30)	2.57×10^7	3.96×10^5	-3.46
Monsoon (7/1 to 9/30)	2.12×10^7	1.47×10^5	-4.13
Fall (10/1 to 12/31)	1.09×10^7	1.53×10^5	-3.54
Cerro Paranal Averages for 1993			
1/1 to 2/14	2.42×10^7	5.22×10^5	-3.19
2/15 to 7/31	1.21×10^7	1.68×10^4	-5.46
8/1 to 12/12	2.30×10^7	8.31×10^4	-4.67

Table 3: Average particle counts for Sacramento Peak in 1996 and Cerro Paranal in 1993. The Paranal averages are from data provided by Sarazin and Giordano (1997).

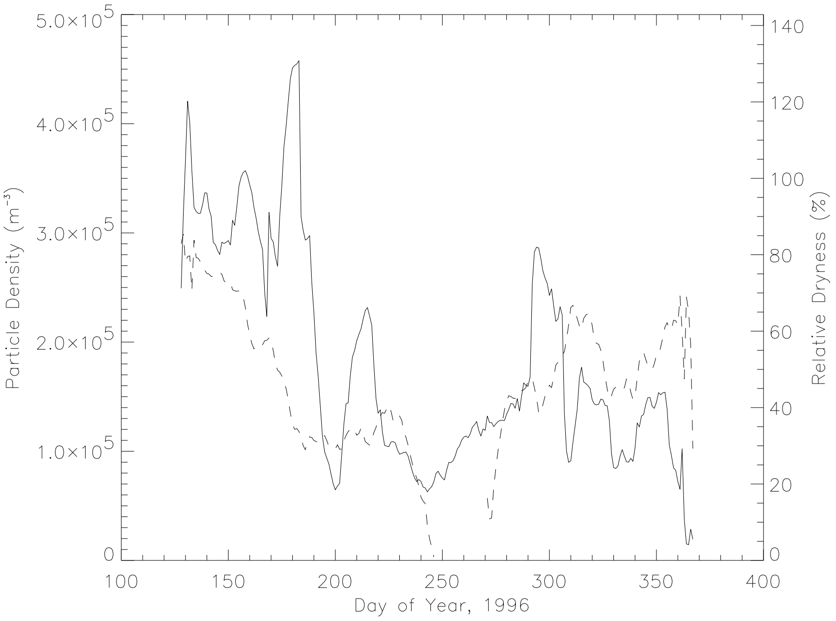

Figure 7: The daily average dust density (solid line) in the $\geq 1.0\mu$m channel, smoothed with a fifteen-day running mean, is shown together with the similarly smoothed value of 100% minus the average relative humidity at Sacramento Peak (dashed line). This quantity, which might be called the "relative dryness", appears to correlate well with the smoothed average dust levels. The gap around day-of-year 260 occured while the weather station was being repaired after being struck by lightning.

as measured at Sacramento Peak and at White Sands Missile Range, about 77 km to the southwest.

The daily average dust density (solid line) in the $\geq 1.0\mu$m channel, smoothed with a fifteen-day running mean, is shown together with the similarly smoothed value of 100% minus the average relative humidity at Sacramento Peak (dashed line) in Figure 7. This quantity, which might be called the "relative dryness", appears to correlate well with the smoothed average dust levels. A plausible explanation for this is that the primary component of the dust seen at Sacramento Peak during dust events is probably made up of gypsum sand from the White Sands National Monument, which is near White Sands Missile Range. As the air dries, the gypsum particles, which are hygroscopic, become less "sticky" and more likely to be lifted by the wind. Thus dust events are more likely when the air is dry.

Comparison of the raw dust counts, as well as the particle size distribution with the coronal sky brightness data from the Evans facility may give empirical information about the size of dust grains that contribute most to sky brightness. Earlier work (Menzel and Sen, 1962) suggests that particles around 1μm diameter are most significant. The observers at the Evans facility record the sky brightness at 0.1 solar radii above the solar disk at noon each clear day. These data are taken with a optical photometer (Evans, 1948). The data indicate that while low sky brightness and low dust level occur together, high sky brightness does not imply a high dust level. This probably indicates that a substantial part of the dust affecting the sky brightness is well above the surface of the ground.

3.4 The Surface Dust Experiment

Figure 8 is not an image of a starfield. Rather, it is the dust on a mirror surface photographed using dark field illumination. In other words, what you are seeing is the light scattered by the dust grains on the surface into the microscope objective. The smallest grains are about 2 microns in size. The dark area at the top of the frame is a piece of black tape over the CCD window providing a black reference for the video camera used to obtain the image. Since the microscope slides are glued to a metal bracket for mounting on the telescope and are not perfectly perpendicular to the microscope optical axis, in order to avoid focus problems only the center portion of each video frame is used.

Figure 9 is the particle size distribution obtained by averaging six fields similar to the above image. These were obtained from an aluminized microscope slide that was exposed for several weeks in May and June 1996 adjacent to the Apache Point Observatory 3.5m primary mirror.

3.5 Modeling the surface particle size distribution

There appear to be two types of size distribution, those which can be modeled by a simple power law, and those which cannot. If all of the available size distributions are modeled with a power law, one obtains the following plot of power law index versus dust cross section (see Figure 10). This indicates that for dirty mirrors (cross section greater than $\sim 10\%$) one can model the particle size distribution as a power law with the index decreasing from around 1.5 down to 0.9 for the dirtiest mirrors. However, the situation of the cleaner mirrors is more complicated. Here, while some distributions (e.g. Figure 11) can be modeled by a steep power law, others, while the fitting function may yield a shallow power law curve, are not really fit well by a power law distribution.

The cleaner mirrors appear to be fit better by a distribution similar to that used by MIL-STD-1246A to define surface cleanliness levels.

$$\log n_L = 0.926[(\log x_1)^2 - (\log x)^2]$$

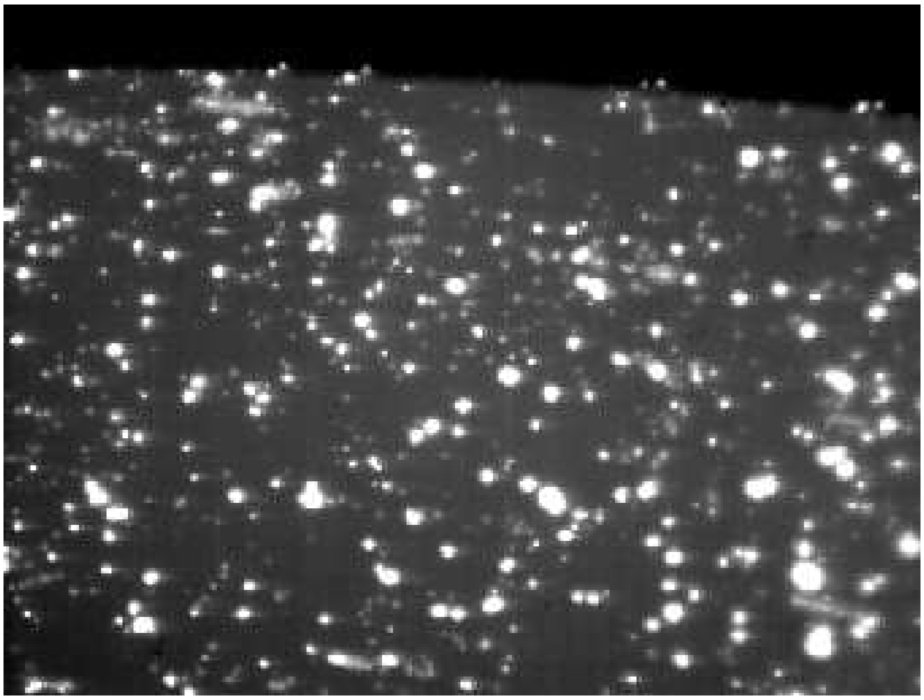

Figure 8: Dark field image of dust on an aluminum-coated microscope slide. Slide exposed for several weeks adjacent to the Apache Point 3.5m telescope primary mirror. Magnification approximately 100×. The black area at the top of the image is where a piece of black tape was mounted over the CCD window to provide a black reference. This area is not included in the particle density calculation.

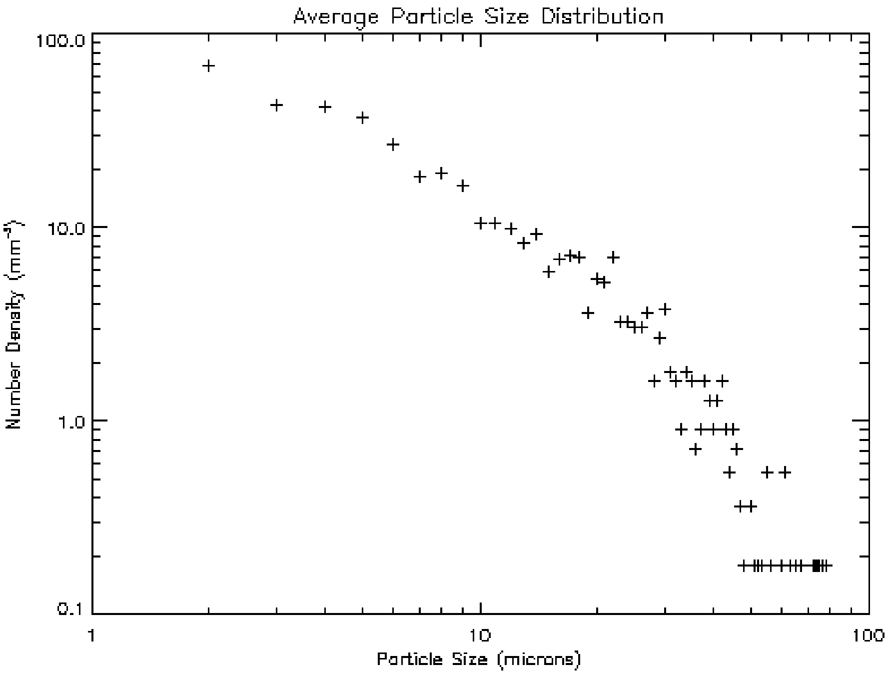

Figure 9: Particle size distribution obtained from Figure 6.

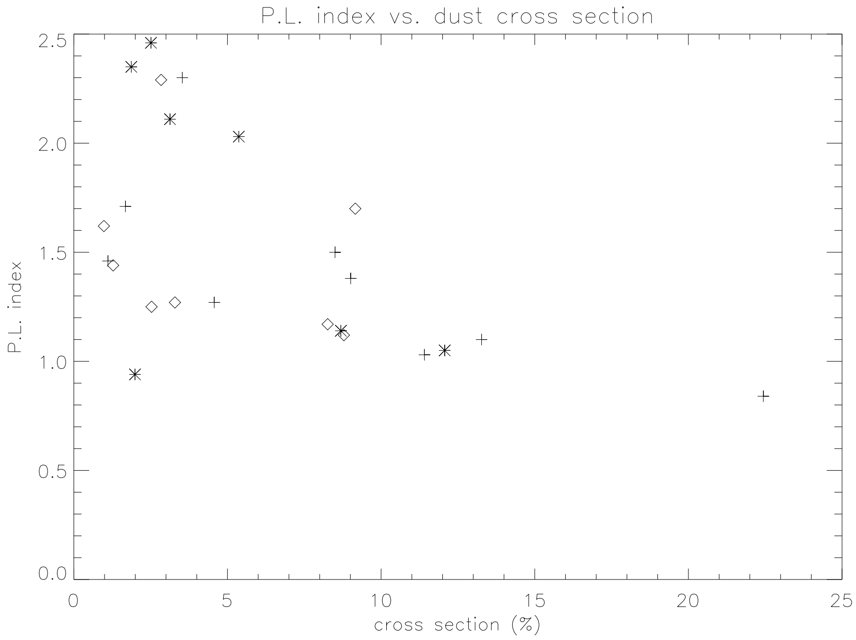

Figure 10: Power-law index versus dust cross section, 1996.

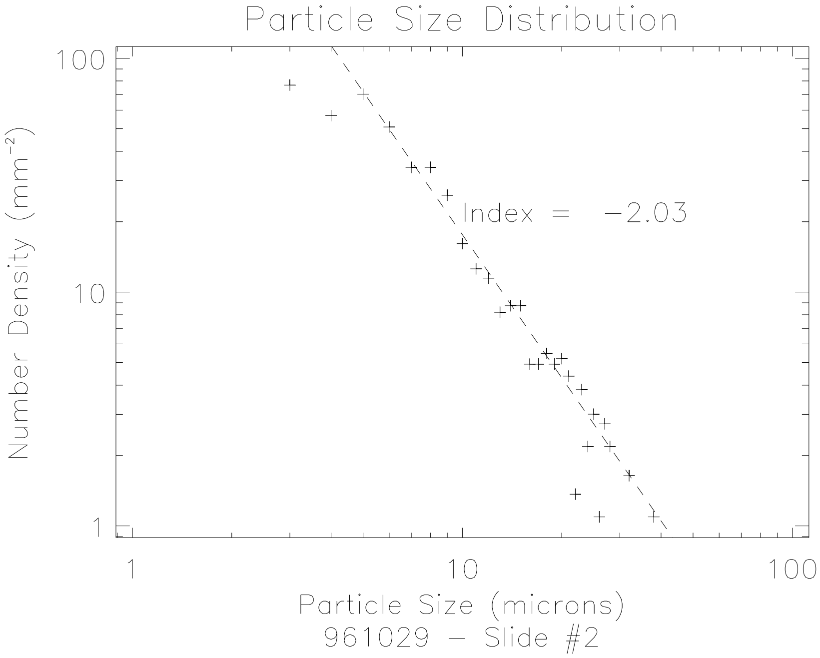

Figure 11: Particle size distribution for Slide #2, measured on October 29, 1996. The slide was exposed on the APO 3.5m telescope beginning October 24. The exposure time (time with the mirror covers open) was 20.5 hours.

Cutoff level (1.0μm channel)	Fraction of dust avoided	Fraction of time closed
3.5×10^5	0.484	0.126
5.3×10^5	0.326	0.058
7.1×10^5	0.228	0.028
8.8×10^5	0.178	0.016
1.06×10^6	0.141	0.009
1.24×10^6	0.118	0.005
1.41×10^6	0.108	0.004

Table 4: Estimated fraction of dust exposure avoided for differing dust cutoff levels. Note that the average dust concentration in the $\geq 1.0\mu$m channel for June 1996 was $4.3 \times 10^5 \mathrm{m}^{-3}$.

Here, n_L is the number of particles with diameter greater than or equal to x (in particles per square foot of surface), x is in microns, and x_1 is the cleanliness level. This standard is commonly used in the aerospace industry to characterize the cleanliness of optical surfaces. Hamberg, quoted in Buch and Barsh (1987), indicates that this distribution was determined for recently cleaned surfaces, and that the value 0.926 should be replaced by 0.383 for surfaces exposed to clean room air for some time.

4 Discussion

4.1 Observing Limits for Airborne Dust

Perhaps the best way to avoid excessive scattering from mirror surfaces due to deposition of dust is to prevent the dust from falling onto the mirror surface. While an experiment is underway on a possible telescope design to reduce dust deposition (see below), the simplest approach to surface dust prevention is to protect the surface during dust events. This adds another criterion to those normally used for closing telescopes (i.e. clouds, high winds, humidity, precipitation). The question here is what dust level to use, so as to avoid the most dust and lose the least observing time.

We have already seen that there is a reasonable correspondence between a dust concentration of $1.24 \times 10^6 \mathrm{m}^{-3}$ in the $\geq 1\mu$m channel and visible dust. By using an airborne dust counter, a limit lower than the point at which dust becomes visible can be chosen. Table 4 shows the fraction of the total dust exposure (based on the May 7 to December 31 data) which can be avoided by covering a telescope mirror when a given dust concentration in the $\geq 1\mu$m channel is exceeded.

In order to avoid losing too much observing time from any one month, a cutoff level of $7.1 \times 10^5 \mathrm{m}^{-3}$ appears reasonable for the Sacramento Peak area.

From the May to December data, we estimate that $\sim 3\%$ of total observing time would have been lost if the telescope were closed at that dust concentration, while $\sim 23\%$ of the total dust exposure would have been avoided. In actuality the time lost would have been less, since some dust events occur during cloudy weather or during other conditions which would have required closing the telescope.

4.2 The resulting scattering from a dusty surface

Experiments (Young 1976, Spyak and Wolfe 1992a,b,c,d) show that the scattering from particles sitting on a mirror surface is best modeled by forward scattering from the particles followed by a specular reflection from the mirror surface. For particles large compared to the wavelength of the light under consideration (which is the case for nearly all the particles measured in the surface dust experiment), according to Babinet's principle the amount of energy removed from the incoming beam by the particles on a mirror should be equal to $2XAI_0$ where X is the fraction of the mirror covered by dust (the "dust cross section" referred to in earlier sections) and A is the area of the mirror. Half of this removed energy is due to Fraunhofer diffraction. The nature of the other half depends on the particles. The energy could be reflected, refracted, or absorbed by the particles. In any case it is removed from the specular beam. For mostly transparent dust grains, the primary effect would be due to refraction. The Fraunhofer diffraction results in scattering at small angles relative to the specular reflection, while the refraction results in large-angle scattering. The proportion of energy lost in small- to large-angle scattering should be roughly 1:1.

4.3 Mirror Throughput Estimates

APO estimates of the throughput of the 3.5-m mirrors have been based on measurements using a Microscan scatterometer (SMS, Portland OR). It may be that these measurements include a component of the scattered light, in addition to reflected light. The result is an overestimate of the reflectivity of these optics by perhaps 10% per surface.

Our measurements of the particle size distribution suggest that the particles between 30 and 40 microns in diameter are the dominant scattering contaminates on dirty mirrors. These particles remove light in two ways. As tiny bits of (mostly) transparent silicate crystals, they refract and reflect light over a fairly large angles. By disturbing the wavefront, they defract light over a solid half angle of lambda/diameter of about 1 degree.

The Microscan has an aperture of about 1 mm about 30 mm from the surface. Thus, it appears to include light over a solid half-angle of 1 degree or more as reflected. Consequently, it may count diffracted light as reflected (plus a bit of the refracted light). The diffracted light will not enter a spectrograph slit because of its very small solid angle.

How big is the effect? If the Microscan measures 80% reflectivity, i.e., 10% loss from the coating and 10% detected scattering, the actual scattering may be 20% and the actual reflectivity 70%. For two surfaces, the reflectivity may be 49% rather than 64%. This is a significant effect.

The important point here is that the Microscan scatterometer (and perhaps other reflectometers) includes small-angle scattering in its reflectivity measurements. This is also noted in an article by Magrath and Nahrstedt (1996).

4.4 Results from the Surface Dust Experiment and Small Angle Scattering

We now examine the contribution made by different size particles to small angle scattering. For large particles and small scattering angles, the only significant term in the intensity distribution from scattering is the Fraunhofer scattering. Since this is true the composition of the particles is not significant and the scattered intensity is given by (van de Hulst 1957):

$$I = \frac{G^2}{\lambda^2 r^2} I_0 D^2$$

with D given by

$$D = \frac{2J_1(x \sin\theta)}{x \sin\theta}$$

with $x = 2\pi a/\lambda$, where a is the radius of the particle r is the distance from the particle to the observer, and G is the cross-sectional area of the particle. Since we are concerned with small angles we can approximate $x\sin\theta$ by $x\theta$. For values of $x\theta$ small (so that J_1 is well within its first zero), D can be replaced by the truncated series:

$$D = 1 - \frac{(x\theta)^2}{8}$$

. Squaring D and dropping the $(x\theta)^4$ term leads to:

$$I = \frac{G^2}{\lambda^2 r^2} I_0 (1 - \frac{(x\theta)^2}{4})$$

.

For the situation where θ is small, the intensity of the scattering is nearly constant. Since we are near normal incidence the Bidirectional Reflectance Distribution Function (BRDF) is then given by

$$BRDF = n(y)\frac{G^2}{\lambda^2},$$

where n is the number density of particles and G is the cross-sectional area of the particles. We note that the first zero of J_1 occurs at 1.7^o for 20μm diameter particles at a wavelength of 0.5μm. For smaller particles the first zero is farther out.

If we assume a power-law particle size distribution such that the dust cross section is given by:

$$X = \int Cy^{-p} \frac{\pi y^2}{4} dy$$

or

$$X = \frac{\pi C}{4} \frac{y_{max}^{3-p}}{3-p}.$$

The scattering is given by:

$$BRDF_{mirror} = \int Cy^{-p} \frac{\pi^2 y^4}{16\lambda^2} dy$$

or

$$BRDF_{mirror} = \frac{C\pi^2}{16\lambda^2} \frac{y_{max}^{5-p}}{5-p}$$

or

$$BRDF_{mirror} = \frac{\pi}{4\lambda^2} y_{max}^2 \frac{3-p}{5-p} X$$

or

$$BRDF_{mirror} = \frac{G_{max}}{\lambda^2} \frac{3-p}{5-p} X.$$

4.5 Emissivity of the Dust-Covered Surface

Experiments on the total hemispherical emissivity of contaminated surfaces (Facey and Nonnenmacher, 1988) suggest that the total emissivity is given by

$$\epsilon = \epsilon_m + kx$$

where ϵ_m is the emissivity of the clean mirror coating and x is the dust cross section of the mirror. The value of k was found to be about 0.5. This would produce emissivity levels for our test samples (assuming a typical emissivity for aluminum of 0.02) of between 0.02 and 0.13. The dust is usually the largest contributor to the emissivity, even with aluminum coatings.

Fortunately an air filter that is effective at some particle diameter tends to be more effective for larger diameter particles.

Dust Cross Section (%)	y_{max} (μm)	BRDF	Scatter (millionths)
0.13	2	0.008	0.56
0.5	2	0.031	2.15
0.5	5	0.20	13.5
0.5	10	0.78	53.9
1.0	5	0.40	27.0

Table 5: Estimated contributions to the solar aureole from dust on the primary mirror surface of a reflecting coronagraph, in millionths of the solar disk brightness. We assume the focal length of the telescope is 12m, the pixel size of the detector is 20μm, and the size distribution of the dust obeys a function of the form $n(y) = Cy^{-p}$, where y is the particle diameter and $p = 1$. The wavelength of the light used is 0.5μm.

5 Conclusion: Implications for CLEAR Design

If we assume $p = 1$, focal length = 12m, pixel size = 20μm we can estimate the contribution to the solar aureole from dust on the surface of the primary mirror. See Table 5. In making this estimate we assume the angular distribution of the scattered light is constant (Equation nn above) and that all parts of the solar disk contribute the same amount (in other words we don't include the effect of limb darkening).

Although reducing the overall number of particles is important in limiting the scatter from dust, it is at least as important to limit the particle size. The large particles are very effective scatterers.

From comparison of the Cerro Paranal data and the airborne dust counts from Sacramento Peak, it appears that there can be significant variation in the number of large ($\geq 1.0\mu$m) particles present in the air at different sites. Since these particles have the largest effect on small-angle scattering when they have settled on optical surfaces, the choice of an observing site can make a significant difference in telescope scattered light performance, emissivity, and throughput.

5.1 The dust deposition rate

In a series of tests between 20 August and 15 October slides were exposed for several weeks (though not consecutively) without cleaning. During this period the airborne dust counts were generally uniform and low. The $\geq 1.0\mu$m channel typically showed a density of $\sim 1.8 \times 10^5$m^{-3} while the $\geq 0.3\mu$m channel showed a density of $\sim 1.8 \times 10^7$m^{-3}. The dust accumulations suggest that a typical accumulation rate under these conditions is $\sim 0.07\%$ hr^{-1}.

Other test series indicate that there is a wide variation in accumulation rates, from 0.01%hr^{-1} to 0.17%hr^{-1}, or more than a factor of 10. See Table 6.

Clearly the deposition of dust on large coronagraphic telescopes must be actively controlled. One method of doing this could be to place the primary

Date (1996)	Exp. time (hr)	Net cross section gain (%)	Deposition rate (% hr^{-1})
8/20 - 8/27	15.4	2.42	0.157
8/27 - 9/3	16.1	1.55	0.096
9/3 - 9/10	30.7	1.86	0.061
9/10 - 9/17	20.8	0.76	0.036
9/17 - 9/26	58.3	4.97	0.085
10/1 - 10/15	97.7	5.50	0.056
10/24 - 10/29	20.5	3.50	0.171
11/6 - 11/25	227.4	2.89	0.013

Table 6: Dust deposition rate on the APO 3.5m sample slides.

mirror in an enclosure in which a slight overpressure of clean, filtered air is maintained. Such an enclosure should prevent most dust particles from collecting on the primary mirror. An experiment using a 1/7 scale mock-up of the proposed CLEAR telescope is underway which should provide some indication of whether this is a workable idea.

6 Acknowledgements

We would like to thank the Sloan Digital Sky Survey and APO for providing the dust counter and access to their weather mast and computer facilities. We would like to thank Mark Klaene of APO for providing the test slides and mounting them on the telescope for us.

7 References

Beckers, J. M. (1996) *Solar Physics*, submitted.
Buch, J. D., and Barsh, M. K. (1987) *SPIE* **777**, 43.
Evans, J. W., (1948) *J.O.S.A.* **38**, 1083.
Facey, T. A., and Nonnenmacher, A. L. (1988) *SPIE* **967**, 308.
Giordano, P. and Sarazin, M. (1994) *SPIE* **2199**, 977.
Kimura, W. D., Kim, G. H., and Balick, B. (1995) *PASP* **107**, 888.
Kormandy, J. (1973) *AJ* **78**, 255.
Kuhn, J. (1997) private communication.
Magrath and Nahrstedt (1996) *PASP* **108**, 620.
McClatchey, R. A., Fenn, R. W., Selby, J. E. A., Volz, F. E., and Garing, J. S. (1978) in *Handbook of Optics*, ed. W. G. Driscoll and W. Vaughan, McGraw-Hill: New York, pg. 14-3.
Menzel, D. H. and Sen, H. K. in *Proceedings of the Symposium on Solar Seeing*, 1962, Consiglio Natzionale delle Ricerche: Roma, pg. 67.

MIL-STD-1246A, *Product Cleanliness Level and Contamination Control Plan*, August 1967.
Sarazin, M., and Giordano, P. (1997), private communication.
Spyak, P. R., and Wolfe, W. L. (1992a) *Optical Engineering* **31** 1746.
Spyak, P. R., and Wolfe, W. L. (1992b) *Optical Engineering* **31** 1756.
Spyak, P. R., and Wolfe, W. L. (1992c) *Optical Engineering* **31** 1764.
Spyak, P. R., and Wolfe, W. L. (1992d) *Optical Engineering* **31** 1775.
van de Hulst, H. C. (1947) *ApJ* **105**, 471.
van de Hulst, H. C. (1957) *Light Scattering by Small Particles*, Wiley: New York, pg. 106.
Young, R. P. (1976) *Optical Engineering* **15**, 516.